Journal of Science Research International (JSRI)
ISSN: 2456-6365 (Online)

OPEN ACCESS

SYNTHESIS AND CHARACTERIZATION OF $NIFE_2O_4$/WFS SAND FOR ADSORPTION STUDY

Chandrashekhar Patil, Jyoti Bote, Ram Shirvadekar, Sanket Sathe, Satish Patil and Uttam Chougale*

PG Department of Chemistry,

Karmaveer Hire Arts, Science, Commerce and Education College, Gargoti, Maharashtra, India 416 209

**Corresponding author E-mail: uttamchougale1985@gmail.com*

Received: 25 January 2025	Revised: 13 March 2026	Accepted: 22 March 2026	Published: 30 March 2026

DOI: **https://doi.org/10.5281/zenodo.19369648**

Abstract:

A magnetic nanocomposite of nickel ferrite ($NiFe_2O_4$) based on Waste Foundry Sand (WFS) was created in order to effectively adsorb Methylene Blue (MB) dye from aqueous solutions. Because WFS is a substantial industrial waste with significant percentages of SiO2, Al_2O_3, and Fe_2O_3, it was utilized as a sustainable substrate. A straightforward co-precipitation technique was used to create the $NiFe_2O_4$@WFS composite, which was then examined using XRD, FTIR, and SEM-EDX. Adsorption experiments were used to demonstrate MB removal.

Keywords: *Ni-Fe_2O_4, Waste Foundry Sand Support, Adsorption, MB Dye Removal.*

1. Introduction

The distribution of unprocessed textile waste containing Methylene Blue (MB) presents a significant environmental risk due to its toxicity and limited biodegradability [1,2]. Due to its high effectiveness and low cost, adsorption is a suggested cleanup technique [3,4]. This study explores a "waste-to-wealth" strategy using Waste Foundry Sand (WFS) as the basis for magnetic $NiFe_2O_4$ composites.This composite not only overcomes the WFS disposal problems but also provides a magnetically recoverable adsorbent for water treatment [5,6].

2. Materials and Methods

2.1. Preparation of Waste Foundry Sand (WFS)

WFS was collected from a local foundry and subjected to thorough washing with deionized water to remove soluble impurities, followed by drying at 105 °C for 24 h.

2.2. Synthesis of $NiFe_2O_4$@WFS composite

The composite was prepared using a modified co-precipitation

i. ***Solution preparation*:** Stoichiometric amounts of $NiNO_3.6H_2O$ and $FeCl_3.6H_2O$ (molar ratio 1:2) were dissolved in deionized water.

ii. ***Impregnation:*** A known mass of treated WFS was added to the precursor solution and stirred vigorously to ensure uniform dispersion [7].

iii. ***Precipitation:*** 2 M NaOH or ammonia solution was added dropwise until the pH reached ~11 to facilitate the formation of the spinel ferrite phase.

iv. ***Thermal treatment:*** The resulting solid was filtered, washed multiple times, and calcined (e.g., at 500–600 °C) to stabilize the magnetic $NiFe_2O_4$ crystals on the sand matrix [8].

3. Characterization

3.1 X-Ray Diffraction (XRD)

The cubic spinel structure of $NiFe_2O_4$/WFS was confirmed by analysis, with distinctive peaks at approximately 25, 28, 38, 57, 62, and 64 together with the quartz phase from the WFS substrate [9.10].

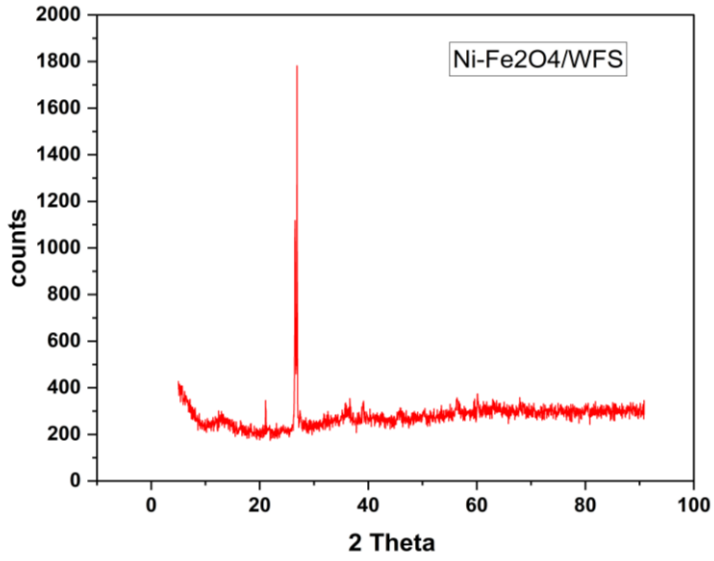

Figure 1: XRD Spectrum of Ni-Fe_2O_4/WFS

3.2 FTIR spectroscopy

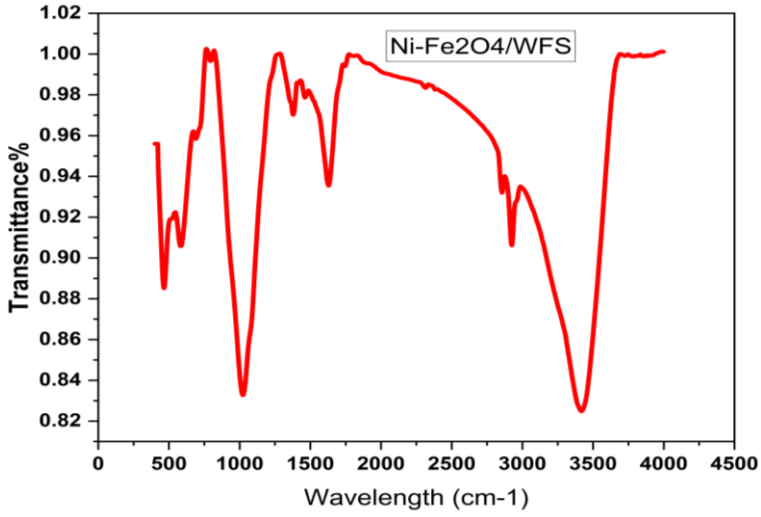

Figure 2: FTIR Spectra of Ni-Fe_2O_4/WFS

The Fe–O stretching vibration in the tetrahedral sites of the spinel structure was identified by the spectra, which showed a peak around 580 cm^{-1}. Important auto peaks at various wavelengths, such as 465, 580, 690, 794, 1023, 1378, 1462, 1629, 1743, 2314, 2855, 2924, 3417 cm−1, are visible in the spectra, exhibiting spectrum characteristics of Ni-Fe_2O_4/WFS [11,12].

3.3 Raman analysis

In NiFe2O4/WFS (Nickel Ferrite/Waste Foundry Sand) composites, Raman analysis usually detects the structural contributions from the WFS support and verifies the emergence of the spinel ferrite phase. The synthetic composite has significant peaks at 155, 325, 680, and 1313 cm-1. The symmetric stretching of oxygen atoms in relation to metal ions (Fe-O and Ni-O) is responsible for the strongest peak, which is located between 680 and 705. caused by the asymmetric bending of Fe/Ni (~330 cm^{-1}) and oxygen. (~200–210 cm^{-1}) is the source of the symmetric bending of oxygen atoms with respect to the metal ion [13].

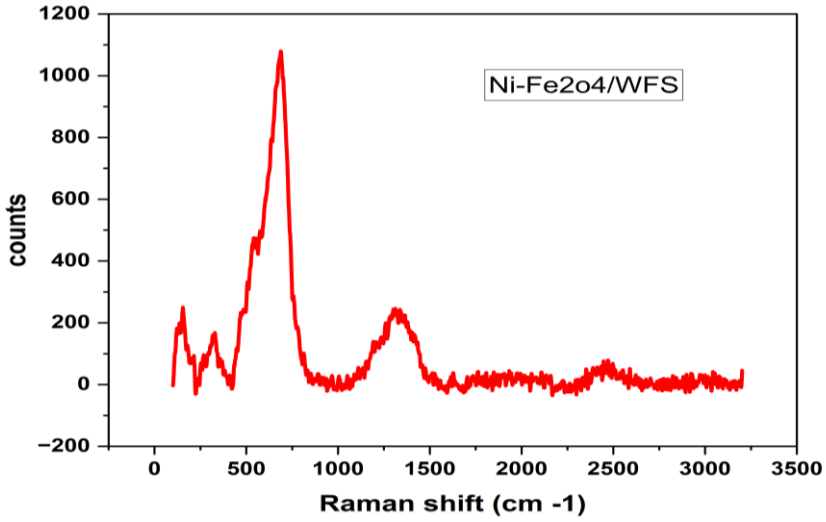

Figure 3: Raman Spectra of Ni-Fe_2O_4/WFS

4. Adsorption studies

4.1. Batch adsorption experiments

By performing batch sorption tests in a 250 mL flask with 100 mL of MB solution and shaking at 150 rpm, the study investigated the effectiveness of MB dye removal. The goal was to identify the ideal ranges for several sorption parameters, including the starting dye concentration (5–50 mg/L), adsorbent dose (0.1–0.3 g/100 mL), pH (8), working solution temperature (25–35 °C), and adsorption duration (0–120 min). To confirm the results, the average triplicate runs and the other parameters were held constant while one parameter was examined at a time. Following each run, the spent adsorbent was separated using centrifugation, and the concentration of the solute in the supernatant was determined using the following equations at the UV–VIS spectrophotometer's λmax of 663 nm [1] and [2].

$$\%\text{Removal} = Co - Ce\ Co * (100) \quad \text{.....(1)}$$

$$qe = (Co - Ce)\ m * V \quad \text{.....(2)}$$

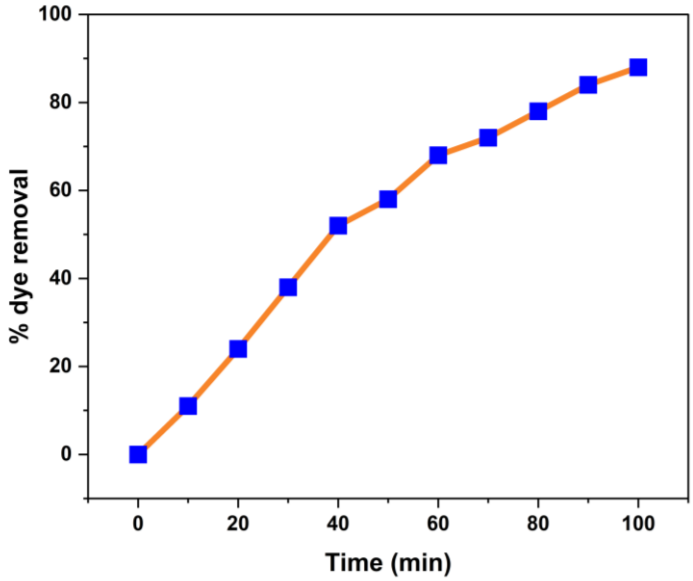

Figure 4: Adsorption of MB dye on Ni-Fe_2O_4/WFS composite with time

4.2. Effect of pH

The pH of the solution is essential since it regulates both the dye's ionization and the adsorbent's surface charge. For the cationic dye Methylene Blue, adsorption usually increases as pH increases from acidic to basic. At low pH, high concentrations of (H+) ions compete with the dye molecules for accessible adsorption sites, and the positively charged surface repels the cationic dye, which lowers removal rates.

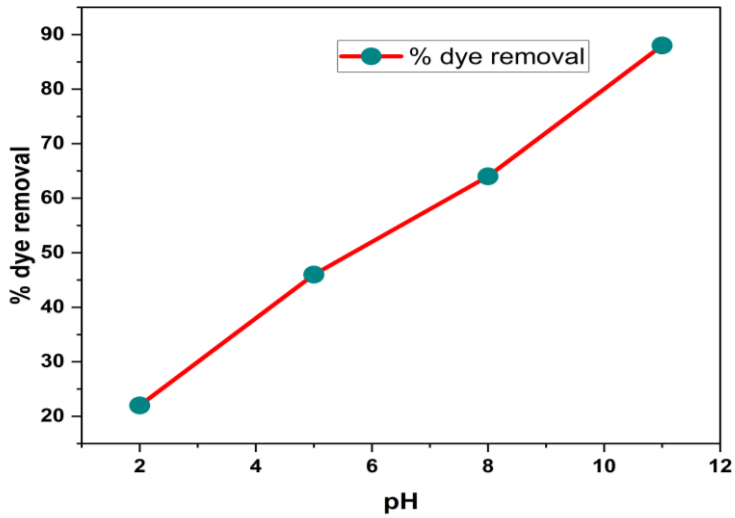

Figure 5: Effect of pH MB dye adsorption on Ni-Fe_2O_4/WFS composite

4.3 Effect of initial dye concentration

The initial concentration of the dye provides the driving force to overcome mass transfer resistance between the aqueous and solid phases. While the total amount adsorbed (%) goes up, the overall percentage of dye removed usually decreases at very high concentrations. This is because the available active sites on the adsorbent surface become saturated, leaving more dye in the solution.

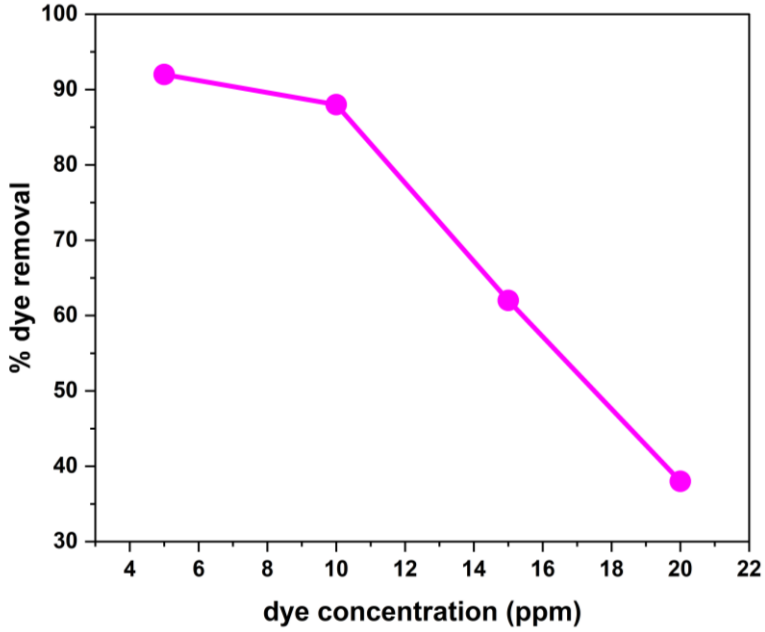

Figure 6: Effect of initial concentration MB dye adsorption on Ni-Fe_2O_4/WFS composite

4.4 Recycle study

The recyclability of NiFe2O4/WFS (Nickel Ferrite/Waste Foundry Sand) composites for Methylene Blue (MB) adsorption is primarily driven by the material's magnetic properties and surface stability, which allow for efficient recovery and multiple reuse cycles. Many NiFe composites maintain near 90-80 % removal efficiency even after 4 to 5 successive cycles.

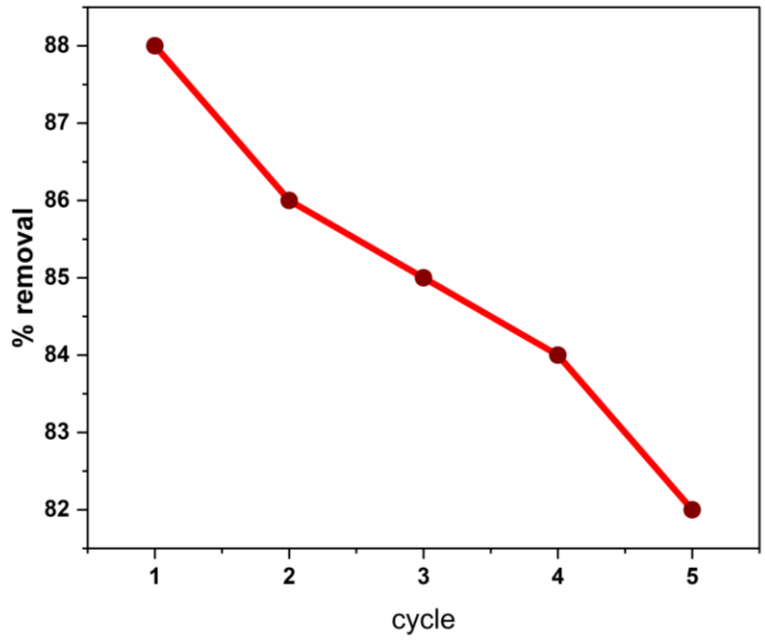

Figure 7: Recyclability Ni-Fe_2O_4/WFS composite of MB dye adsorption

Conclusion

The $NiFe_2O_4$-supported WFS composite acts as an effective, sustainable, and magnetically separable adsorbent for Methylene Blue. The integration of industrial waste (WFS) with magnetic nanoparticles not only enhances the surface area but also facilitates easy post-treatment recovery.

References

1. Chiban, M., Zerbet, M., Carja, G., & Sinan, F. (2012). Application of low-cost adsorbents for arsenic removal: A review. *Journal of Environmental Chemistry and Ecotoxicology, 4*(5), 91–102.
2. Dehghani, M. H., *et al.* (2024). Sustainable remediation technologies for removal of pesticides as organic micro-pollutants from water environments: A review. *Applied Surface Science Advances, 19*, 100558.
3. Dehghani, M. H., Najafpoor, A., & Azam, K. (2010). Using sonochemical reactor for degradation of LAS from effluent of wastewater treatment plant. *Desalination, 250*(1), 82–86.
4. Asghari, F. B., Mohammadi, A. A., Dehghani, M. H., & Yousefi, M. (2018). Data on assessment of groundwater quality with application of ArcGIS in Zanjan, Iran. *Data in Brief, 18*, 375.
5. Qureshi, S. S., *et al.* (2022). Microwave-assisted synthesis of carbon nanotubes for the removal of toxic cationic dyes from textile wastewater. *Journal of Molecular Liquids, 356*, 119045.
6. Nikfar, E., *et al.* (2016). Removal of bisphenol A from aqueous solutions using ultrasonic waves and hydrogen peroxide. *Journal of Molecular Liquids, 213*, 332–338.
7. Gupta, V. K. (2009). Application of low-cost adsorbents for dye removal–a review. *Journal of Environmental Management, 90*(8), 2313–2342.
8. Praveen, S., Jegan, J., Bhagavathi Pushpa, T., Gokulan, R., & Bulgariu, L. (2022). Biochar for removal of dyes in contaminated water: An overview. *Biochar, 4*(1), 10.
9. Bansal, S., Pandey, P. K., & Upadhayay, S. (2021). Methylene blue dye removal from wastewater using *Ailanthus excelsa* Roxb as adsorbent. *Water Conservation Science and Engineering, 6*(1), 1–9.
10. Farooq, S., *et al.* (2022). Synthesis and characterization of copper oxide-loaded activated carbon nanocomposite: Adsorption of methylene blue, kinetic, isotherm, and thermodynamic study. *Journal of Water Process Engineering, 47*, 102692.
11. Pervez, M. N., Hassan, M. M., & Naddeo, V. (2024). Separation of cationic methylene blue dye from its aqueous solution by S-sulfonated wool keratin-based sustainable electrospun nanofibrous membrane biosorbent. *Separation and Purification Technology, 333*, 125903.
12. Mousavi, S. A., Mahmoudi, A., Amiri, S., Darvishi, P., & Noori, E. (2022). Methylene blue removal using grape leaves waste: Optimization and modeling. *Applied Water Science, 12*(5), 112.
13. Robles-Melchor, L., *et al.* (2021). Removal of methylene blue from aqueous solutions by using nance (*Byrsonima crassifolia*) seeds and peels as natural biosorbents. *Journal of Chemistry, 2021*(1), 5556940.